JURNAL

by Jurnal_pa Nurhadi Buat Pak Gb_5

Submission date: 23-Jan-2019 03:04PM (UTC+0700)
Submission ID: 1067425978
File name: Titania-Loaded_Coal_Char_as_Catalyst_in_Oxidation.pdf (3.13M)
Word count: 6489
Character count: 32313

Mukhamad Nurhadi, Sheela Chandren, Lai Sin Yuan, Chin Siong Ho, Teuku Meurah Indra Mahlia and Hadi Nur*

Titania-Loaded Coal Char as Catalyst in Oxidation of Styrene with Aqueous Hydrogen Peroxide

DOI 10.1515/ijcre-2016-0088

Abstract: Titania-loaded coal char catalyst was successfully prepared. The preparation steps involved pyrolysis of low rank coal at different temperatures and durations, sulfonation, impregnation of titanium(IV) isopropoxide, and then heating at 110 °C. It is found that the coal chars' surfaces were rough after sulfonation and impregnation, while large pore volume, high surface area and carbon composition were observed at low pyrolysis temperature for short duration. These properties contributed to high selectivity towards benzaldehyde (> 90 %) at 600 °C (0.5–2 h)) in styrene oxidation using aqueous hydrogen peroxide as the oxidant.

Keywords: titania-loaded coal char, styrene, oxidation, sulfonation, aqueous hydrogen peroxide

1 Introduction

The catalytic oxidation of styrene over titania impregnated on many supports has been a focus of investigation in fundamental chemistry and modern industrial processes, as epoxides are important building blocks in organic synthesis (Zhan et al. 2009). Many commercial products can be created from epoxides compounds acting as the intermediates, such as perfumes, anthemintics, epoxy resins, plasticizers, drugs, sweeteners, chiral pharmaceuticals, pesticides, and epoxy paints (Zhan et al. 2009; Qi et al. 2010).

Many researches have been carried out on different approaches to utilize titania impregnated on various supports in the oxidation of styrene with hydrogen peroxide as the oxidant. The catalysts that have been used are TS-1 (Zhuang et al. 2004; Uguina et al. 2000), Ti-beta (Corma, Esteve, and Martinez 1996), Ti-MCM-41 (Lin et al. 2009), Ti-LHMS-3 (Modak, Nandi, and Bhaumik 2012), V-Ti-MCM-41 and Nb-Ti-MCM-41 (Parvulescu et al. 2003). These catalysts exhibited high catalytic activity and selectivity. However, these kinds of catalysts are very expensive for extensive application.

Herein, an alternative support has emerged, via carbon resource. Carbon is a common material utilized as a support precursor due to its unique characteristic such as inexpensiveness, inertness and stability. Carbon support can increase the dispersion of the active phases, control the porous structure, improve mechanical strength, prevent sintering and assist catalysis (Satterfield 1980). There are many types of materials which can be used as carbon source. Currently, coal is one of the most important carbon source. This is because coal possesses many advantages such as its chemical composition being dominated by carbon, cheap and easily available (Song and Schobert 1996); Lazaro et al. 2008).

Coal char is the material formed when raw coal is pyrolysed at high temperature (Peter et al. 1988). Coal char composes mainly of carbon and mineral matter. Coal chars have large pores, high internal surface area and high reactivity in oxidation reactions. Coal char could be used as a possible alternative and a new kind of economical support for catalysts (Chern and Hayhurst 2011).

In this study, low cost coal char has been utilized as the support material for the catalysts. The catalysts were prepared by sulfonation of coal char from low rank coal, followed by impregnation of titania from titanium(IV) isopropoxide. The sulfonation of coal char was carried out by using concentrated sulfuric acid that is able to

*Corresponding author: Hadi Nur, Centre for Sustainable Nanomaterials, Ibnu Sina Institute for Scientific and Industrial Research, Universiti Teknologi Malaysia, 81310 UTM Skudai, Johor, Malaysia, E-mail: hadi@kimia.fs.utm.my
Mukhamad Nurhadi, Department of Chemical Education, Universitas Mulawarman, Kampus Gunung Kelua, Samarinda, 75119, East Kalimantan, Indonesia
Sheela Chandren, Centre for Sustainable Nanomaterials, Ibnu Sina Institute for Scientific and Industrial Research, Universiti Teknologi Malaysia, 81310 UTM Skudai, Johor, Malaysia; Department of Chemistry, Faculty of Science, Universiti Teknologi Malaysia, 81310 UTM Skudai, Johor, Malaysia
Lai Sin Yuan, Southern University College, Jalan Selatan Utama, Off Jalan Skudai, 81300 Skudai, Johor, Malaysia
Chin Siong Ho, Low Carbon Asia Research Center, Faculty of Built Environment, Universiti Teknologi Malaysia, 81310 UTM Skudai, Johor, Malaysia
Teuku Meurah Indra Mahlia, Department of Mechanical Engineering, Universiti Tenaga Nasional, Kajang 43000, Selangor, Malaysia

form oxygen functional groups, such as SO_3H, COOH and OH groups in a three-dimensional network of the material. The oxygen functional groups in the material's surface provide good access for titania active sites to be incorporated as catalyst. In the catalytic process, incorporation of oxygen functional groups on the materials' surface also provides good access of reactant to the SO_3H groups and titania active sites, which gives rise to high catalytic performance, despite the small surface area. The catalytic performance of this material was tested out in the oxidation of styrene with 30% aqueous hydrogen peroxide as the oxidant at room temperature.

2 Experimental

2.1 Raw materials

Low rank coal from Batuah, Loa jannan, Kutai Kartanegara East Kalimantan, Indonesia was used as the raw material.

2.2 Pyrolysis process

The coal char supported catalysts were prepared from pyrolysed low rank coal. The low rank coal was pulverized to 200 meshes before undergoing pyrolysis. Pyrolysis was carried out in a stainless steel reactor in a vertical furnace under nitrogen atmosphere with a gas flow rate of 100 cm^3/min. Different pyrolysis temperatures were used (600, 700, 800 and 900 °C) with heating rate of 5 °C/min and maintained for 0.5 h. In order to investigate the effect of the duration of pyrolysis, pyrolysis at 600 °C was also done for 0.5, 1 and 2 h. The coal chars obtained after pyrolysis were labeled as CC-X (Y), where CC stands for coal char, X is the pyrolysis temperature and Y as the duration of pyrolysis. For instance, CC-600(0.5) represents coal char that was obtained after pyrolysis at 600 °C for 0.5 h.

2.3 Sulfonation and impregnation process

The sulfonation of coal char was carried out by using sulfuric acid (6 ml, 98%, JT Baker) per gram of coal char. The mixture was stirred intermittently in an oil bath at 90 °C for 6 h. Subsequently, the mixture was washed with distilled water to remove any loosely-bound acid. It was then dried overnight at 110 °C (Mittal and Venkobachar 1996). Sulfonated coal char is denoted as SO_3H/CC-X-Y. For example, SO_3H/CC-700 (1.0) represents the coal char that was obtained after pyrolysis at 700 °C for 1 h followed by sulfonation. After sulfonation, impregnation of titania was done by using 500 µmol of titanium(IV) isopropoxide (97%, Aldrich) dissolved in toluene (Merck). Sulfonated coal char (2 g) was immersed and stirred intermittently in the toluene containing the titania source until all the toluene was completely evaporated. After that, the solid was washed by using ethanol to remove any remaining toluene and dried at 110 °C. The catalysts obtained were labeled as Ti-SO_3H/CC-X-Y. For example, Ti-SO_3H/CC-700(0.5) represents sulfonated coal char which was pyrolysed at 700 °C for 0.5 h and impregnated with titania by using 500 µmol of titanium(IV) isopropoxide. The list of catalysts prepared and their codes are listed in Table 1.

Table 1: Codes and treatments done to the samples.

Samples	Type of treatment	Time of sulfonation (h)	Temperature of pyrolysis (°C)	Time of pyrolysis (h)
CC-600(0.5)	–	–	600	0.5
SO_3H/CC-600(0.5)	Sulfonation	6	600	0.5
Ti-Coal	–	–	–	–
Ti-CC-600 (0.5)	–	–	600	0.5
Ti-SO_3H/CC-600(0.5)	Sulfonation	6	600	0.5
Ti-SO_3H/CC-600(1.0)	Sulfonation	6	600	1.0
Ti-SO_3H/CC-600(2.0)	Sulfonation	6	600	2.0
Ti-SO_3H/CC-700(0.5)	Sulfonation	6	700	0.5
Ti-SO_3H/CC-800(0.5)	Sulfonation	6	800	0.5
Ti-SO_3H/CC-900(0.5)	Sulfonation	6	900	0.5

2.4 Samples characterization

Catalysts were characterized by Fourier transform infrared (FTIR) spectroscopy using a Thermo Scientific Nicolet iS50, with a spectral resolution of 4 cm^{-1}, scans of 16 s, at temperature of 20 °C. Crystallinity and phase content of the solid materials were investigated using a Bruker AXS Advance D8 X-ray difractometer (XRD) with the Cu K_α ($\lambda = 1.5406$ Å) radiation as the diffracted monochromatic beam at 40 kV and 40 mA. The patterns were scanned in the 2θ range of between 5° and 80°, at a step of 0.03° and step time of 1 s. Field emission scanning electron microscope (FE-SEM) images and mapping elements were determined by using the JSM-6701F which has high resolution FE-SEM and energy dispersive X-ray analyzer (EDX) JEOL-JED 2300. The hydrophobicity of all catalysts was determined using the water adsorption technique (Nur et al. 2005). In a typical experiment, samples (0.1 g) were dried in an oven at 110 °C overnight to

remove all physically adsorbed water. Distilled water (0.75 l) was filled into desiccators for overnight. After dehydration, the samples were exposed to water vapor by placing them into the water-filled desiccators at room temperature and weighed every 30 min. The percentage of adsorbed water as a function of time was determined by $((m_t - m_o)/m_o)) \times 100\,\%$, where mt represents the sample mass after adsorption of water and mo represents the initial mass of the sample (Nur et al. 2005). Nitrogen adsorption–desorption isotherms were measured at 77 K using a Micromaritics ASAP 2020 V4.00 instrument. The apparent surface areas were calculated from the nitrogen adsorption data, using the Brunauer-Emmett-Teller equation, utilizing data in the 0.01–0.2 relative pressure range. The total pore volume was obtained from the amount of N_2 adsorbed at the relative pressure of 0.975. The micropore volume was determine using t-Plot method. The pore size distributions (PDS) based on the nitrogen isotherms were calculated by applying the Barrett-Joyner-Halenda (BJH) model with the use of BJH Desorption Dv(d). Samples were degassed at 150 °C for 12 h prior to analysis.

2.5 Catalytic test

The catalytic activities of the prepared catalysts were tested out in the oxidation of styrene with aqueous H_2O_2 (30 %, Merck) as the oxidant. Styrene (5 mmol, Aldrich), aqueous H_2O_2 (5 mmol, 30 %, Merck), acetonitrile (4.5 ml, Merck) and catalyst (100 mg) were mixed in a sample bottle and stirred at room temperature for 20 h (Zhan et al. 2007, 2009). The products were then separated from the catalysts by centrifugation. A portion of the resulting liquid mixture was withdrawn and analyzed by GC-2014 Shimadzu-gas chromatograph equipped with a BPX5 column (30 m × 0.25 mm × 0.25 µm), a flame ionization detector (FID) and nitrogen as the carrier gas. The temperatures of the injector.and detector were programmed at 250 and 260 °C, respectively. The temperature of the column oven was programmed to increase from 80 to 140 °C, at a rate of 10 °C/min.

3 Results and discussion

3.1 Physical properties

The coal rank was determined as lignite from the proximate and ultimate analysis. The proximate and ultimate analysis is presented in Table 2.

Table 2: Proximate analysis result of the low rank coal.

Proximate analysis		Ultimate analysis	
Moist (%)	13.67		
Ash (%)	4.10	C (%)	65.4
VM (%)	37.99	H (%)	4.88
FC (%)	46.0	N (%)	1.16
TS (%)	0.26	O (%)	12.29
Cal. Val (Kcal/Kg)	6,342		

Notes: Moist = moisture content, Ash = ash content, VM = volatile matter content, FC = fixed carbon content, TS = total sulfure content, Cal val = calorific value, C = carbon, H = hydrogen, N = Nitrogen, O = oxygen.

Figure 1(a)–(h) shows the XRD patterns of the modified coal chars prepared, *i. e.* CC-600(0.5), SO_3H/CC-600(0.5), Ti-SO_3H/CC-600(0.5), Ti-SO_3H/CC-600(1.0), Ti-SO_3H/CC-600 (2.0), Ti-SO_3H/CC-700(0.5), Ti-SO_3H/CC-800(0.5) and Ti-SO_3H/CC-900(0.5). The weak and broad diffraction peak at 2θ value of 10–30° (C (200)) assigned to amorphous carbon

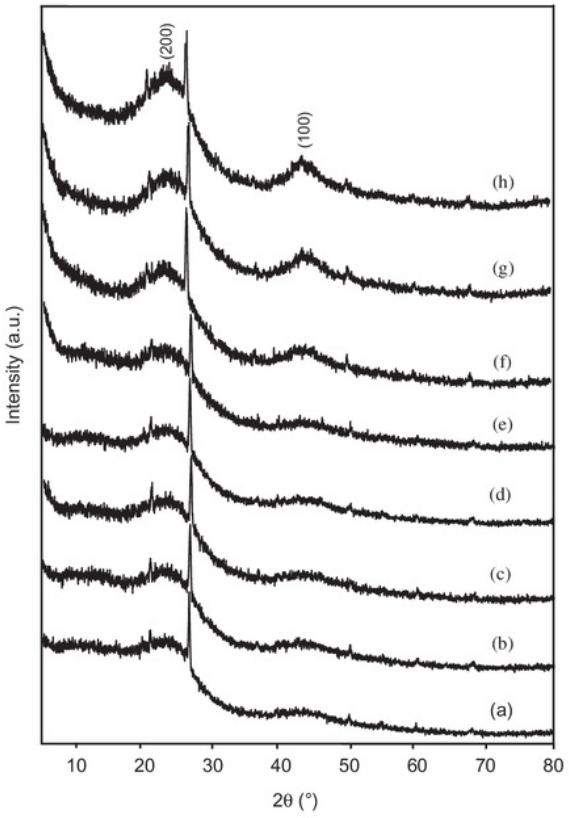

Figure 1: XRD patterns for (a) CC-600(0.5) (b) SO_3H/CC-600 (0.5) (c) Ti-SO_3H/CC-600(0.5) (d) Ti-SO_3H/CC-600 (1.0) (e) Ti-SO_3H/CC-600 (2.0), (f) Ti-SO_3H/CC-700(0.5), (g) Ti-SO_3H/CC-800(0.5) and (h) Ti-SO_3H/CC-900(0.5).

composed of aromatic carbon sheets can still be observed (Liu et al. 2009). All samples showed a sharp crystalline peak at 2θ value of 26.5°, which is assigned to quartz (Nurhadi et al. 2015). The broad and weak peaks at 2θ value of 35–50° are assigned to turbostratic graphite structure (Peng et al. 2010). These peaks are used to investigate low rank coal that has been pyrolysed at different time durations and temperature. All the patterns appeared similar, indicating that the different time durations, 0.5–2.0 h, that has been used during pyrolysis, do not have much influence on the structure of the coal char. The graphite peak is relatively small for the low rank coal pyrolysed at 600 °C and when the temperature of pyrolysis was increased, it become more prominent and sharper (Liu et al. 2009; Hasegawa et al. 2010)

The FTIR spectra for CC-600(0.5), SO_3H/CC-600(0.5), Ti-SO_3H/CC-600(0.5), Ti-SO_3H/CC-600(1.0), Ti-SO_3H/CC-600 (2.0), Ti-SO_3H/CC-700(0.5), Ti-SO_3H/CC-800(0.5) and Ti-SO_3H/CC-900(0.5) are shown in Figure 2. The FTIR spectra of all samples show a broad band at 3,416 cm^{-1}, which is assigned to the O-H stretching mode of the –COOH and phenolic OH groups (Peng et al. 2010). It is generally known that if the transmittance is high, the amount of the functional group present in the sample is low. According to the transmittance data it can be predicted the amount of OH groups in samples is in the increasing order as follows: CC-600(0.5) < SO_3H/CC-600(0.5) < Ti-SO_3H/CC-600(0.5) ~Ti-SO_3H/CC-600(1.0) ~ Ti-SO_3H/CC-600(2.0) ~ Ti-SO_3H/CC-700 (0.5) ~ Ti-SO_3H/CC-800(0.5) ~ Ti-SO_3H/CC-900(0.5). The OH groups increased after sulfonation and titania impregnation processes because titanol (Ti-OH) groups were created. The characteristic of aromatic C = C stretching mode in polyaromatics and graphite-like materials are shown in the vibration band at 1,619 cm^{-1}. The $-SO_3H$ groups attached on the coal chars surface are indicated by the vibrations at 1,034 cm^{-1} and 571 cm^{-1}. The peak at 1,034 cm^{-1} is assigned to the presence of S = O symmetric stretching mode and the SO_2 deformation frequency, while C-S stretching mode is detected in the region of 571 cm^{-1}. These peaks proved the existence of covalent bond between the sulfonic acid groups and coal chars surface (Peng et al. 2010). The existence of titanium framework was characterized by an adsorption band in the region of 900–975 cm^{-1}. The peak at approximately 966 cm^{-1} in Ti-SO_3H/CC-600(0.5) and Ti-SO_3H/CC-700(0.5) is attributed to Ti-O-Si on the surface of sulfonated coal char (Duprey et al. 1997; Prasad et al. 2008; Nur 2006). In Ti-SO_3H/CC-800(0.5) and Ti-SO_3H/CC-900(0.5), the adsorption band in the region 900–975 was undetected due to the overlapping of the broad silanol groups Si-OH peak with the region peak of Ti-O-Si. The silica linkages can be detected by the adsorption band at 1,094 cm^{-1} and 795 cm^{-1}

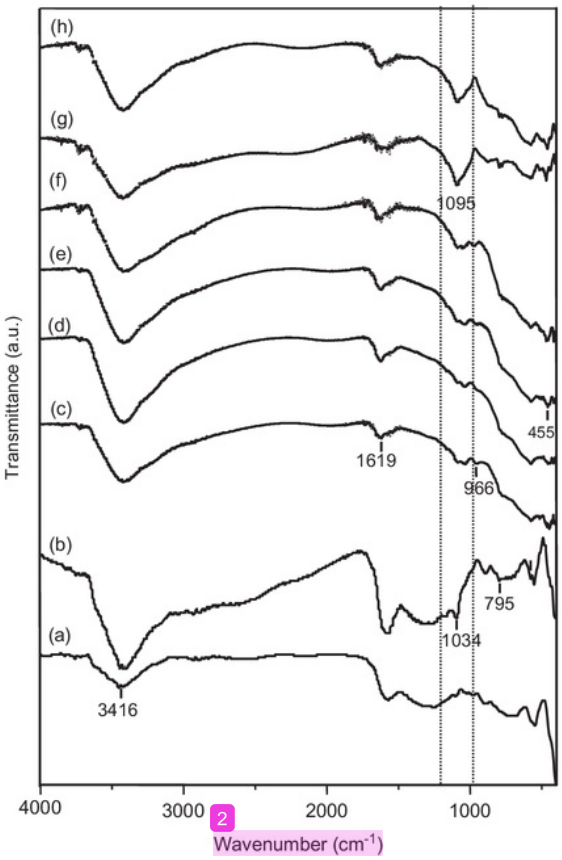

Figure 2: FTIR spectra of (a) CC-600(0.5) (b) SO_3H/CC-600 (0.5) (c) Ti-SO_3H/CC-600(0.5) (d) Ti-SO_3H/CC-600 (1.0) (e) Ti-SO_3H/CC-600 (2.0), (f) Ti-SO_3H/CC-700(0.5), (g) Ti-SO_3H/CC-800(0.5) and (h) Ti-SO_3H/CC-900(0.5).

(Prasad et al. 2008; Duprey et al. 1997; Nur 2006; Nur, Hayati, and Hamdan 2007). It is worth noting that the amount of silanol groups increased when the pyrolysis temperature increased. The peak at 455 cm^{-1} is attributed to the symmetric O-Ti-O stretching that is caused by the vibration of Ti-O bond.

The N_2 adsorption-desorption isotherms and corresponding pore size distribution curves (using the BJH method) for Ti-SO_3H/CC-600(0.5), Ti-SO_3H/CC-600 (1.0), Ti-SO_3H/CC-600(2.0), Ti-SO_3H/CC-700(0.5), Ti-SO_3H/CC-800(0.5) and Ti-SO_3H/CC-900(0.5) are shown in Figure 3 (A) and (B), respectively. All the isotherms are of type V with type H-3 hysteresis loops (Leofanti et al. 1998) in the relative pressure range of 0.3–0.99 for Ti-SO_3H/CC-600(0.5), Ti-SO_3H/CC-600(1.0) and Ti-SO_3H/CC-600(2.0), 0.45–0.99 for Ti-SO_3H/CC-700(0.5), 0.5–0.99 for Ti-SO_3H/CC-800(0.5) and 0.7–0.99 for Ti-SO_3H/CC-900(0.5). The BET

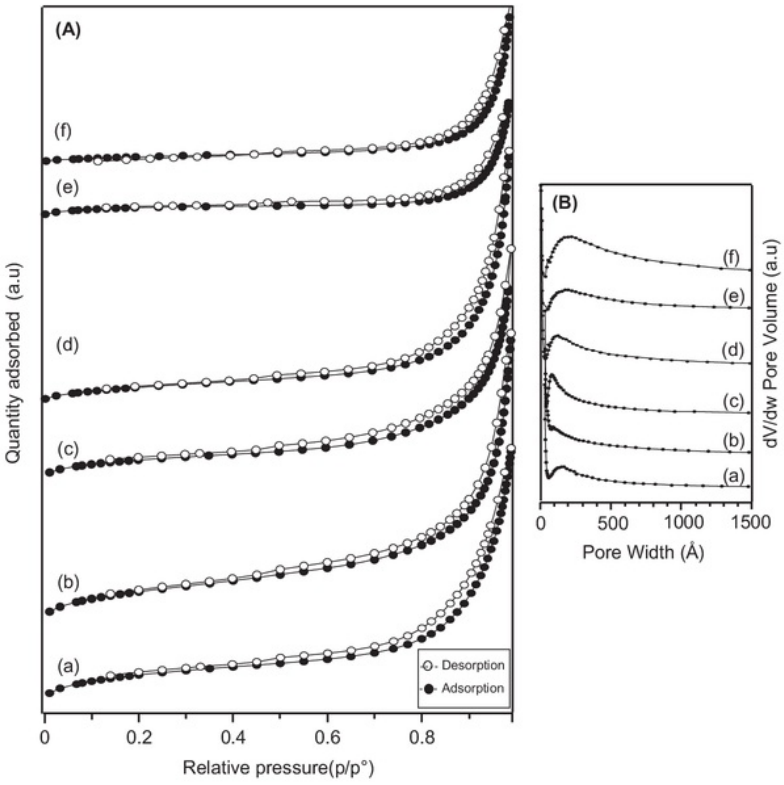

Figure 3: (A) N_2 adsorption-desorption isotherms and (B) BJH pore size distribution of (a) Ti-SO_3H/CC-600(0.5), (b) Ti-SO_3H/CC-600(1.0), (c) Ti-SO_3H/CC-600(2.0), (d) Ti-SO_3H/CC-700(0.5), (e) Ti-SO_3H/CC 800(0.5), and (f) Ti-SO_3H/CC-900(0.5).

surface area, the total pore volume and pore size showed the following values; 17.4 m^2g^{-1}, 0.046 cm^3g^{-1}, 13.7 nm (Ti-SO_3H/CC-600(0.5)), 18.4 m^2g^{-1}, 0.053 cm^3g^{-1}, 14.6 nm (Ti-SO_3H/CC-600(1.0)), and 12.9 m^2g^{-1}, 0.042 cm^3g^{-1}, 19.7 nm (Ti-SO_3H/CC-600(2.0)), 11.9 m^2g^{-1}, 0.045 cm^3g^{-1}, 22.6 nm (Ti-SO_3H/CC-700(0.5)), 9.1 m^2g^{-1}, 0.02 cm^3g^{-1}, 27.4 nm (Ti-SO_3H/CC-800(0.5)) and 5.4 m^2g^{-1}, 0.02 cm^3g^{-1}, 29.6 nm (Ti-SO_3H/CC-900(0.5)), respectively. It can be seen that the BET surface area was influenced by the duration of pyrolysis. The BET surface area, pore volume and pore size increased slightly when the duration of pyrolysis was 1 h and decreased when the duration was increased to 2 h. Removal of carbon atoms from the original coal during pyrolysis for 1 h led to the increase in the average pore size and opening of closed pores. However, when the pyrolysis was done for 2 h, the collapsing of the pores may have contributed to the decrease in surface area. These results also showed that increasing the pyrolysis temperature of low rank coal led to the decrease in BET surface area and the total pore volume, while increasing the average pore size of the samples. Increasing the temperature of pyrolysis can cause the carbon structure inside the coal to be destroyed and undergo change; namely releasing many atomics carbon from the carbon framework as volatile organic compounds, CO_2 and CO. The collapse of pore structure collapsed caused the decrease in surface area of the samples. The complete list of BET surface area, pore volume and mean pore size data is shown in Table 3.

Table 3: Physical properties of the catalysts.

Samples	BET surface area (m^2/g)	Pore Volume (cm^3/g)	Mean pore size (nm)	Average percentage of water adsorption (%wt)
CC-600(0.5)	0.92	0.002	12.72	5.03
SO_3H/CC-600(0.5)	2.35	0.003	13.20	5.47
Ti-Coal	7.74	0.031	22.87	7.46
Ti-CC-600(0.5)	16.88	0.031	13.91	5.49
Ti-SO_3H/CC-600(0.5)	17.39	0.046	13.71	5.41
Ti-SO_3H/CC-600(1.0)	18.41	0.053	14.64	5.23
Ti-SO_3H/CC-600(2.0)	12.86	0.042	19.71	5.22
Ti-SO_3H/CC-700(0.5)	11.93	0.045	22.62	5.81
Ti-SO_3H/CC-800(0.5)	9.10	0.020	27.35	6.22
Ti-SO_3H/CC-900(0.5)	5.42	0.026	29.61	7.28

Figure 4 shows the thermogravimetric analysis curves of (a) Ti-SO_3H/CC-600(0.5), (b) Ti-SO_3H/CC-700 (0.5), (c) Ti-SO_3H/CC-800(0.5) and (d) Ti-SO_3H/CC-900 (0.5). The weight losses of the samples were obtained in two steps. In the first step, the weight loss began at 30 °C, reached midpoint at 46.9 °C, and continued until 100 °C. This step can be associated with the evaporation of adsorbed water on the samples, with Ti-SO_3H/CC-900(0.5) having the highest weight loss of 4.2 %wt. The weight loss in the second step started at 575 °C and ended at 837 °C, with a midpoint of 771 °C. This weight loss was due to the decomposition of organic compounds. The highest total weight loss was shown by Ti-SO_3H/CC-600(0.5) at around 15.6 %wt.

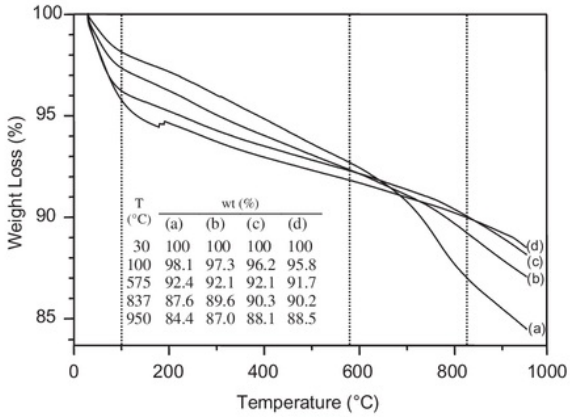

T (°C)	wt (%) (a)	(b)	(c)	(d)
30	100	100	100	100
100	98.1	97.3	96.2	95.8
575	92.4	92.1	92.1	91.7
837	87.6	89.6	90.3	90.2
950	84.4	87.0	88.1	88.5

Figure 4: TGA curves of (a) Ti-SO_3H/CC-600(0.5), (b) Ti-SO_3H/CC-700 (0.5), (c) Ti-SO_3H/CC-800(0.5) and (d) Ti-SO_3H/CC-900(0.5).

Figure 5(a)–(i) shows the FE-SEM and SEM-EDX dot images of Ti-SO_3H/CC-600(0.5), Ti-SO_3H/CC-600(2.0), and Ti-SO_3H/CC-900(0.5). From the FE-SEM images, no obvious differences in morphology can be seen and these particles were clearly agglomerated. As for SEM EDX dot images, it can be seen that Ti-SO_3H/CC-600(0.5) is less homogeneous as compared to Ti-SO_3H/CC-600(2.0) and Ti-SO_3H/CC-900(0.5).

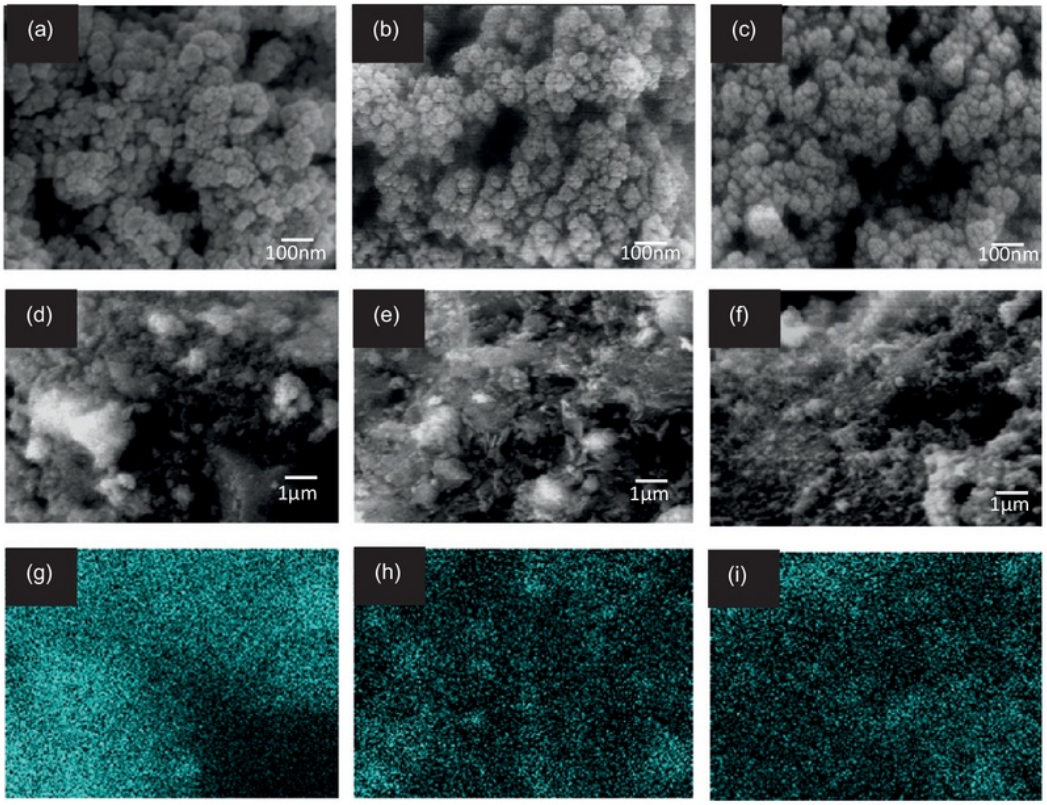

Figure 5: FE SEM/EDX images of Ti-SO_3H/CC-600(0.5) catalyst (a, d, g), Ti-SO_3H/CC-600(2.0) catalyst (b, e, h) and Ti-SO_3H/CC-900(0.5) catalyst (c, f, i). The bright dot and areas are Ti.

Figure 6 shows the EDX spectra of Ti-SO_3H/CC-600 (0.5), Ti-SO_3H/CC-600(2.0) and Ti-SO_3H/CC-900(0.5). It could be seen that all of the spectra showed the elements peak of C, O, Si, Al, S and Ti. The complete percentage of all the elements is listed in Table 4. Samples Ti-SO_3H/CC-600 (0.5), Ti-SO_3H/CC-600(2.0), and Ti-SO_3H/CC-900(0.5) contained almost similar percentage of titania, as the amount of titania impregnated for all three samples was 500 µmol. The amount of $-SO_3H$ groups attached on the coal char's surface can be predicted from the percentage of S element in the EDX analysis. The percentage of S element decreases when the duration and temperature of pyrolysis increased, with the following trend: Ti-SO_3H/CC-600(0.5) > Ti-SO_3H/CC-600 (2.0) > Ti-SO_3H/CC-900(0.5). The percentage of C element also decreased when time duration and temperature of pyrolysis increased. On the other hand, the percentage of Si element increased when the duration and temperature of pyrolysis increased.

Table 4: Elementals obtained using EDX.

Variable	Samples	Elements					
		C	O	Al	Si	S	Ti
Temperature	Ti-SO_3H/CC-600(0.5)	79.8	12.1	0.5	1.1	0.9	4.3
	Ti-SO_3H/CC-900(0.5)	60.3	16.2	3.6	13.9	0.4	4.9
Time	Ti-SO_3H/CC-600(0.5)	79.8	12.1	0.5	1.1	0.9	4.3
	Ti-SO_3H/CC-600(2)	57.6	16.8	4.8	15.2	0.7	4.1

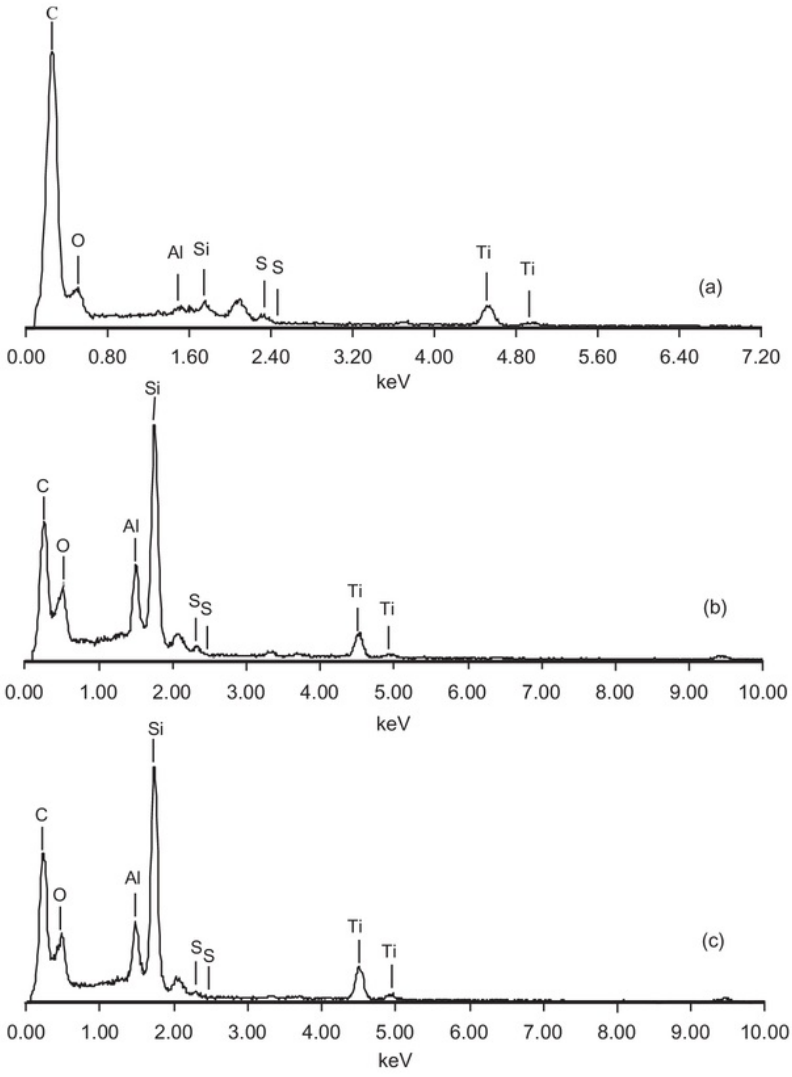

Figure 6: EDX spectra of (a) Ti-SO_3H/CC-600(0.5), (b) Ti-SO_3H/CC-600(2.0) and (c) Ti-SO_3H/CC-900(0.5).

Table 3 shows the amount of adsorbed water for samples CC-600(0.5), SO_3H/CC-600(0.5), Ti-Coal, Ti-CC-600(0.5), Ti-SO_3H/CC-600(0.5), Ti-SO_3H/CC-600(1.0), Ti-SO_3H/CC-600(2.0), Ti-SO_3H/CC-700(0.5), Ti-SO_3H/CC-800(0.5) and Ti-SO_3H/CC-900(0.5). The amount of adsorbed water corresponds to the hydrophobicity of the samples. The lower the amount of water adsorbed, the higher the hydrophobicity of the samples. From the results, it can be seen that the sulfuric acid treatment and titania impregnation processes influence the amount of adsorbed water. The sulfuric acid treatment caused increase in the average amount of adsorbed water (CC-600(0.5) to SO_3H/CC-600(0.5) 5.03 to 5.47 % wt). The sulfuric acid treatment also caused significant changes in the surface chemistry of the coal char (CC). Sulfuric acid solution produced oxygenated functional groups (SO_3H, COOH and OH groups), CO_2 and CO, which caused the catalyst's surface to become hydrophilic (Izquierdo et al. 2001; Prasad et al. 2008). The impregnation of titania also caused an increase in the percentage of adsorbed water in the samples. Titania impregnation led to changes in oxygen functional groups, with the addition of titanyl (Ti = O) and titanol (Ti-OH) groups on sulfonated coal char's surface, hence increasing the interaction with water.

3.2 Catalytic activity

Benzaldehyde, phenylacetaldehyde, and styrene oxide are important chemical intermediates in fine chemical industry, which are usually produced by the selective oxidation of styrene with H_2O_2 as an oxidant. Styrene oxide (SO) is the primary product expected from the epoxidation of the double bond in the styrene's side chain (Uguina et al. 2000). However, benzaldehyde and styrene oxide are the main product observed in the oxidation of styrene catalyzed by titania supported on modified coal char catalyst. Generally, benzaldehyde is formed by the ring-opening reaction of styrene oxide.

The yield of products from the oxidation of styrene catalyzed by titania supported on modified coal char is shown in Table 5. For comparison, no catalyst, CC-600 (0.5), SO_3H/CC-600(0.5), Ti-Coal and Ti-CC-600(0.5) were also used as the catalysts for this reaction. The yield of benzaldehyde was very low (0.008 mmol) when no catalyst was used. The yield almost did not change when CC-600(0.5) was used as the catalyst, indicating that CC-600(0.5) has low catalytic activity in this reaction. SO_3H/CC-600(0.5) exhibited a rather high

Table 5: Catalytic performance of the catalysts in the oxidation of styrene[a].

Catalyst	Styrene conversion (%)	Yields of product (mol)		
		BzA[b]	PhA[c]	SO[d]
No catalyst	0.3	0.008	0.008	0.005
TiO_2	1.3	0.072	0.011	0.003
CC600(0.5)	0.3	0.006	0.002	0.008
SO_3HCC600(0.5)	0.8	0.010	0.002	0.009
Ti-Coal	3.6	0.169	0.002	0.006
Ti-CC600(0.5)	10.8	0.571	0.005	0
Ti-SO_3HCC600(0.5)	17.1	0.814	0.016	0.042
Ti-SO_3HCC600(1.0)	19.0	0.822	0.005	0.027
Ti-SO_3HCC600(2.0)	17.4	0.821	0.017	0.060
Ti-SO_3HCC700(0.5)	12.9	0.633	0.010	0.030
Ti-SO_3HCC800(0.5)	10.4	0.512	0.007	0.023
Ti-SO_3HCC900(0.5)	9.0	0.449	0.006	0.020

[a] **Reaction conditions:** The reactions were carried out at room temperature for 20 h with styrene (5 mmol), 30 % H2O2 (5 mmol) and catalyst (50 mg). [b]BzA = benzaldehyde, [c]PhA = phenylacetaldehyde, and [d]SO = styrene oxide

catalytic activity with benzaldehyde yield of 0.011 mmol, due to the presence of -SO_3H groups. In order to explain the influence of titania, TiO_2, Ti-Coal and Ti-CC-600(0.5) were also used as catalyst in order to compare with titania supported on sulfonated coal char catalysts. TiO_2 and Ti-Coal had catalytic activity lower than that of Ti-CC-600(0.5), with the benzaldehyde yield of 0.072 mmol, 0.169 mmol and 0.571 mmol, respectively. These enhanced results were caused by the increase in surface area, with the evidence provided by the N_2 adsorption-desorption analysis, which were 0.92 m^2g^{-1}, 7.74 m^2g^{-1} and 16.88 m^2g^{-1}, as shown in Table 3. The yields of benzaldehyde when Ti-SO_3H/CC-600(0.5), Ti-SO_3H/CC-700(0.5), Ti-SO3H/CC-800(0.5) and Ti-SO3H/CC-900 (0.5) were used as catalysts were 0.814 mmol, 0.633 mmol, 0.511 mmol and 0.448 mmol, respectively. The catalytic activity of Ti-SO_3H/CC-600(0.5) was much higher than that of Ti-CC-600(0.5). This is caused by the attachment of -SO_3H groups on CC-600(0.5)'s surface. The catalytic activity of Ti-SO_3H/CC-600(0.5) is much higher than that of Ti-SO_3H/CC-700(0.5), Ti-SO_3H/CC-800(0.5) and Ti-SO_3H/CC-900(0.5). This can be correlated with surface area and hydrophobicity. As shown in Table 3, the coal char obtained at 600 °C has higher total surface area and pore volume than the catalysts that were prepared from coal char with higher temperature of 700, 800 and 900 °C. The reduction of catalytic activity also can be explained based on the decrease in hydrophobicity of Ti-SO_3H/CC-600(0.5), Ti-

SO_3H/CC-700(0.5), Ti-SO_3H/CC-800(0.5) and Ti-SO_3H/CC-900(0.5) catalysts (Table 3). The hydrophobicity trend decreases as follows: Ti-SO_3H/CC-600(0.5) > Ti-SO_3H/CC-700(0.5) > Ti-SO_3H/CC-800(0.5) > Ti-SO_3H/CC-900(0.5). This trend is caused by the decreasing amount of C element and increasing of silanol groups, Si-OH. Furthermore, the existence of hydroxyl groups on Si-OH caused difficulty for the styrene substrate to access the active sites. Moreover, when the surface of the catalyst interacted with the reactant, H_2O_2 will release water as the side product. This will then cause the surface of the catalyst with low hydrophobicity to readily adsorb H_2O, resulting in the poisoning of the catalyst.

Catalysts that were pyrolised at 600 °C but with different durations (0.5 h, 1.0 h and 2.0 h) are labeled as Ti-SO_3H/CC-600(0.5), Ti-SO_3H/CC-600(1.0) and Ti-SO_3H/CC-600(2.0). The varying duration of pyrolysis had no significant effect on the catalytic activity. This phenomenon can be explained by the hydrophobicity test as shown in Table 3. The average amount of adsorbed water on Ti-SO_3H/CC-600(0.5), Ti-SO_3H/CC-600(1.0), and Ti-SO_3H/CC-600(2.0) were 5.40, 5.23 and 5.22%wt, respectively. Therefore, their ability to avoid poisoning by H_2O is almost the same. Hence, the similar activities were shown in the oxidation reaction.

The catalytic performance of catalysts for the oxidation of styrene is also identified through the conversion and products selectivity, which are shown in Table 5 and Figure 7. The results show that CC-600 (0.5), SO_3H/CC-600(0.5) and TiO_2 display lower styrene conversion, which is nearly similar to when no catalyst was used. Using supported Ti-CC-600(0.5) as the catalyst, 10.8% of styrene conversion is achieved, which indicates that the Ti active sites on the surface are somewhat active for the oxidation of styrene. When Ti-SO_3H/CC-600(0.5) was used as the catalyst, higher conversion of styrene is obtained with the main product of benzaldehyde and a little amount of phenylacetaldehyde and styrene oxide. The fact that the conversion of styrene over Ti-SO_3H/CC-600(1.0) is higher than that of over Ti-SO_3H/CC-600(0.5) shows that a higher surface area is crucial in increasing the catalytic activity. The styrene conversion decreased when Ti-SO_3H/CC-700(0.5), Ti-SO_3H/CC-800(0.5) and Ti-SO_3H/CC-900(0.5) were used the catalysts. This is because as the pyrolysis temperature increased, the surface area and hydrophobicity of the catalysts decreased. The selectivity of benzaldehyde for all titania supported on modified coal chars catalysts was more than 90%.

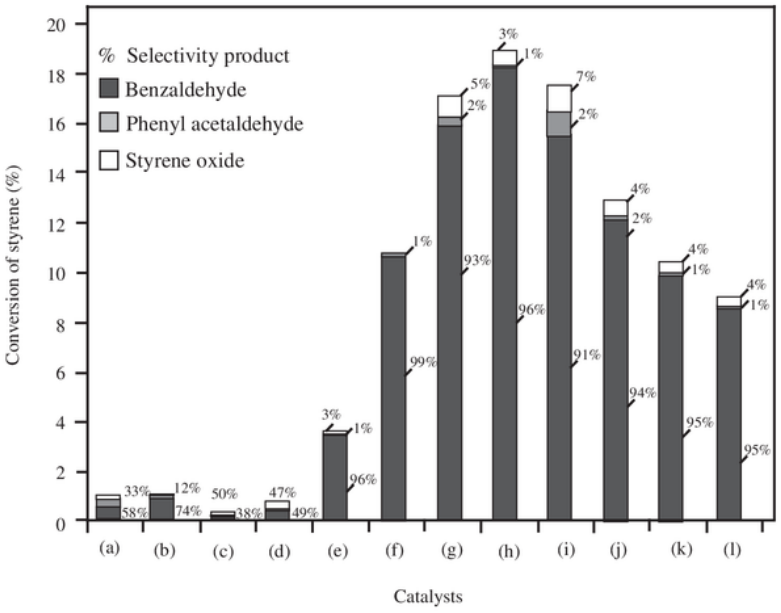

Figure 7: Conversion of styrene and selectivity of the products.

4 Conclusions

Oxidation of styrene by using hydrogen peroxide as the oxidant with coal char catalysts that were prepared at different pyrolysis temperature and durations, have been studied. Coal char was modified by sulfonation, followed by impregnation titania has profound affect on styrene oxidation. The catalytic activity of titania supported on sulfonated coal char in the oxidation of styrene decreased with increasing temperature of pyrolysis, with the coal char prepared at 600 °C being the most active. Otherwise, duration of pyrolysis was insignificant to the catalytic activity. The catalytic activity is not only dependent on the total surface area and pore volume, but also on the functional groups on the catalyst's surface and the chemical nature of the coal char's surface.

Acknowledgements: The authors gratefully acknowledge funding from Universiti Teknologi Malaysia (UTM) through Research University Grant, Development of Low Carbon Scenarios for Asia Region and government of East Kalimantan Province, Indonesia.

References

1. Chern, J.S., Hayhurst, A.N., 2011. Fluidised bed studies of: (i) Reaction-fronts inside a coal particle during its pyrolysis or devolatilisation, (ii) the combustion of carbon in various coal chars. Combustion and Flame 159, 367–375.
2. Corma, A., Esteve, P., Martinez, A., 1996. Solvent effects during the oxidation of olefins and alcohols with hydrogen peroxide on Ti-Beta catalyst: the influence of the hydrophilicity–hydrophobicity of the zeolite. Journal of Catalysis 161, 11–19.
3. Duprey, E., Beaunier, P., Huet, M.A.S., Verduraz, F.B., Fraissard, J., Manoli, J.M., Bregeault, J.M., 1997. Characterization of catalysts based on titanium silicalite, TS-1, by physicochemical techniques. Journal of Catalysis 165, 22–32.
4. Hasegawa, G., Kanamori, K., Nakanishi, K., Hanada, T., 2010. Fabrication of activated carbons with well-defined macropores derived from sulfonated poly(divinylbenzene) networks. Carbon 48, 1757–1766.
5. Izquierdo, M.T, Rubio, B., Mayoral, C., Andres, J.M., 2001. Modifications to the surface chemistry of low-rank coal-based carbon catalysts to improve flue gas nitric oxide removal. Applied Catalysis B, 33, 315–324.
6. Lázaro, M.J., Boyano, A., Gálvez, M.E., Izquierdo, M.T., García-Bordejé, E., Ruiz, C., Juan, R., Moliner, R., 2008. Novel carbon based catalysts for the reduction of NO: influence of support precursors and active phase loading. Catalysis Today 137, 215–221.
7. Leofanti, G., Padovan, M., Tozzola, G., Venturelli, B., 1998. Surface area and pore texture of catalysts. Catalysis Today 41, 207–219.
8. Lin, K., Pascarmona, P.P., Vandepitte, H., Liang, D., van Tendeloo, G., Jacobs, P.A., 2009. Direct room-temperature synthesis of methyl-functionalized Ti-MCM-41 nanoparticles and their catalytic performance in epoxidation. Journal of Catalysis 263, 75–82.
9. Liu, Y., Chen, J., You, J., Zhang, L., Liu, X., 2009. Preparation and properties of sulfonated carbon–silica composites from sucrose dispersed on MCM-48. Chemical Engineering Journal 148, 201–206.
10. Mittal, A.K., Venkobachar, C., 1996. Uptake of cationic dyes by sulphonated coal: sorption mechanism. Industrial & Engineering Chemistry Research 35, 1472–1474.
11. Modak, A., Nandi, M., Bhaumik, A., 2012. Titanium containing periodic mesoporous organosilica as an efficient catalyst for the epoxidation of alkenes. Catalysis Today 198, 45–51.
12. Nur, H., 2006 Modification of titanium surface species of titania by attachment of silica nanoparticles. Materials Science and Engineering: B 133, 49–54.
13. Nur, H., Hayati, F., Hamdan, H., 2007. On the location of different titanium sites in Ti-OMS-2 and their catalytic role in oxidation of styrene. Catalysis Communications 21, 49–54.
14. Nur, H., Manan, A.F.N.A, Wei, L.K. Muhid, MNM, Hamdan, H., 2005. Simultaneous adsorption of a mixture of paraquat and dye by NaY zeolite covered with alkylsilane. Journal of Hazardous Materials 117, 35–40.
15. Nurhadi, M., Efendi, J., Lee, S.L., Mahlia, T.M.I., Chandren, S., Ho, C.S., Nur, H., 2015. Utilization of low rank coal as oxidation catalyst by controllable removal of its carbonaceous component. Journal of Taiwan Institute of Chemical Engineers 46, 183–190.
16. Parvulescu, V., Anastasescu, C., Constantin, C., Su, B.L., 2003. Mono (V, Nb) or bimetallic (V–Ti, Nb–Ti) ions modified MCM-41 catalysts: synthesis, characterization and catalysis in oxidation of hydrocarbons (aromatics and alcohols). Catalysis Today 78, 477–485.
17. Peng, L., Philippaerts, A., Ke, X., Noyen, J.V., Clippel, F.D., Tendeloo, G.V., Jacobs, P.A., Sels, B.F., 2010. Preparation of sulfonated ordered mesoporous carbon and its use for the esterification of fatty acids. Catalysis Today 150, 140–146.
18. Peter, F., Nelson, I., Smith, W., Tyler, R.J., Mackie, J.C., 1988. Pyrolysis of coal at high temperatures. Energy Fuels 2, 391–400.
19. Prasad, M.R., Hamdy, M.S., Mul, G., Bouwman, E., Drent, E., 2008. Efficient catalytic epoxidation of olefins with silylated Ti-TUD-1 catalysts. Journal of Catalysis 260, 288–294.
20. Qi, B., Lu, H., Zhou, D., Xia, Q.H., Tang, Z.R., Fang, S.Y., Pang, T., Dong, Y.L., 2010. Catalytic epoxidation of alkenes with 30 % H_2O_2 over Mn^{2+}-exchanged zeolites. Journal of Molecular Catalysis A 322, 73–79.
21. Satterfield, C. N., 1980. Heterogeneous Catalysis in Practice, McGraw-Hill, New York.
22. Song, C., Schobert, H.H., 1996 Non-fuel uses of coals and synthesis of chemicals and materials. Fuel 75, 724–736.
23. Uguina, M.A., Serrano, D.P., Sanz, R., Fierro, J.L.G., Lopez-Granados, M., Mariscal, R., 2000. Preliminary study on the TS-1 deactivation during styrene oxidation with H_2O_2. Catalysis Today 61, 263–270.
24. Zhan, W., Guo, Y., Wang, Y., Guo, Y., Liu, X., Wang, Y., Zhang, Z., Lu, G., 2007. Synthesis of lanthanum-doped MCM-48

molecular sieves and its catalytic performance for the oxidation of styrene. Journal of Physical Chemistry B 111, 12103–12110.
25. Zhan, W., Guo, Y., Wang, Y., Guo, Y., Liu, X., Wang, Y., Zhang, Z., Lu, G., 2009. Study of higher selectivity to styrene oxide in the epoxidation of styrene with hydrogen peroxide over la-doped MCM-48 catalyst. Journal of Physical Chemistry C 113, 7181–7185.
26. Zhuang, J., Ma, D., Yan, Z., Liu, X., Han, X., Bao, X., Zhang, Y., Guo, X., Wang, X., 2004. Effect of acidity in TS-1 zeolites on product distribution of the styrene oxidation reaction. Applied Catalysis A 258, 1–6.

JURNAL

ORIGINALITY REPORT

3%	2%	1%	0%
SIMILARITY INDEX	INTERNET SOURCES	PUBLICATIONS	STUDENT PAPERS

PRIMARY SOURCES

1	dspace.uniten.edu.my Internet Source	2%
2	Didik Prasetyoko. "Characterization and Catalytic Performance of Niobic Acid Dispersed over Titanium Silicalite", Advances in Materials Science and Engineering, 2008 Publication	1%

Exclude quotes	Off	Exclude matches	Off
Exclude bibliography	On		